



CCUS: 4184874

## Dynamics of Permeability Changes in CO<sub>2</sub> Saturated Brine Injection: An Integrated Modeling Approach

Fatemeh Tale<sup>1(\*)</sup>, Abdulrahman Abdulwarith<sup>1</sup>, Feiyan Chen<sup>2</sup>, Stephen Drylie<sup>2</sup>, Alastair Crombie<sup>2</sup>, and Birol Dindoruk<sup>1</sup>, 1. University of Houston, Department of Petroleum Engineering. 2. Core Laboratories

Copyright 2025, Carbon Capture, Utilization, and Storage conference (CCUS) DOI 10.15530/ccus-2025-4184874

This paper was prepared for presentation at the Carbon Capture, Utilization, and Storage conference held in Houston, TX, 03-05 March.

The CCUS Technical Program Committee accepted this presentation on the basis of information contained in an abstract submitted by the author(s). The contents of this paper have not been reviewed by CCUS and CCUS does not warrant the accuracy, reliability, or timeliness of any information herein. All information is the responsibility of, and, is subject to corrections by the author(s). Any person or entity that relies on any information obtained from this paper does so at their own risk. The information herein does not necessarily reflect any position of CCUS. Any reproduction, distribution, or storage of any part of this paper by anyone other than the author without the written consent of CCUS is prohibited.

---

### Abstract

During CO<sub>2</sub>-saturated brine injection in deep saline aquifers, there is a potential occurrence of formation damage or permeability enhancement. This can be due to the reactive interaction between the injected CO<sub>2</sub>-saturated brine and the formation rock. Therefore, in this study, we aim to provide an integrated model that quantifies the impact of dissolution/precipitation of rock minerals during coupled convective, diffusive, and reactive flow. This study employs an integrated methodology that combines geochemical reactions with continuity equations for brine and rock species, specifically in carbonate formations. This coupling enhances accuracy in modeling the formation damage/stimulation or permeability reduction/enhancement. The subject reactive model captures reaction rates through saturation index evaluation to determine precipitation/dissolution potential. Permeability changes are assessed using the Kozeny-Carman equation coupled with the implicit finite difference method. Experimental procedures were carried out to validate the model output, involving sample preparation, saturation with high-salinity brine, and CO<sub>2</sub>-saturated brine injection. Post-test analyses, including micro-CT scanning and geomechanically testing, offer insights into permeability changes in porous media. The results show that the injection of brine does not have a significant effect on permeability, while the injection of CO<sub>2</sub>-saturated brine into a limestone formation results in the dissolution of calcium carbonate, causing a permeability enhancement by a factor of 2 for a case that was tested (experimentally and numerically). However, in the case of the injection of CO<sub>2</sub>-saturated brine into a dolomite formation, the permeability decreases by 33% due to the participation of magnesium carbonate in the formation. The study emphasizes the injection of CO<sub>2</sub>-saturated brine and its implications for deep saline aquifers, underscoring its relevance to the field of carbon capture, utilization, and storage (CCUS). By manipulating the brine composition and further saturating it with CO<sub>2</sub>, an optimum CO<sub>2</sub>-saturated brine composition can be achieved, leading to desirable operational conditions, and avoiding the risk of formation damage or injectivity losses.

## 1 Introduction

Geological CO<sub>2</sub> storage is considered an essential technique to reduce CO<sub>2</sub> emissions into the atmosphere, addressing the challenges of climate change. CO<sub>2</sub> can be stored in various geological formations, including depleted oil and gas reservoirs, deep saline aquifers, coal beds, and geothermal reservoirs (Abdulwarith et al., 2024a; Abdulwarith et al., 2024b; Ammar et al., 2024; Li et al., 2013). Among these, deep saline aquifers have gained significant attention due to their vast storage capacity and geographical availability (Bachu, 2015). The injection of CO<sub>2</sub>-saturated brine into these aquifers is a critical process that involves complex interactions between the injected fluids, formation brine, and reservoir rock, leading to changes in porosity and permeability. These changes are crucial in determining the injectivity and long-term storage capacity of the aquifers.

The injection process in carbonate formations, such as limestone and dolomite, is particularly complex due to the reactive nature of these rocks. When CO<sub>2</sub> is injected, it dissolves in the brine and the process can be more complex especially when hydrocarbons are present. There are many detailed studies for compositionally complex systems without the presence of flow were covered in open literature by Venkatraman et al. 2017, Ratnakar et al. 2020, Dindoruk et al. 2021, and Ratnakar et al. 2024). Such dissolution can lead to the formation of carbonic acid, which reacts with carbonate minerals. This reaction can lead to mineral dissolution, enhancing porosity and permeability, or precipitation, which can reduce permeability depending on the brine chemistry and rock composition (Addassi et al., 2022; Kampman et al., 2014). Previous studies have shown that calcite dissolution can significantly increase permeability, while dolomite formations may experience permeability reduction due to magnesium carbonate precipitation (Noiriel et al., 2009; Parkhurst and Appelo, 2013).

Most prior research has focused on laboratory experiments and theoretical modeling to understand these permeability changes. Experimental studies involving core flood tests have demonstrated the impact of CO<sub>2</sub>-saturated brine on carbonate rocks, showing variations in dissolution and precipitation patterns based on flow rates and brine composition (Jahediesfanjani et al., 2019). Additionally, reactive transport models, such as those using the PHREEQC geochemical framework, have been employed to simulate these processes, integrating the effects of fluid flow, solute transport, and chemical reactions (Parkhurst and Appelo, 2013; Xu et al., 2004). These models provide valuable insights into the spatial and temporal evolution of porosity and permeability during CO<sub>2</sub> injection.

Recent advances in numerical simulations have highlighted the importance of injection parameters, such as flow rate and brine saturation, in controlling the geochemical interactions within the reservoir. For instance, high flow rates can lead to the formation of preferential flow paths, or "wormholes," which enhance permeability in localized areas but may create challenges for uniform CO<sub>2</sub> distribution. Conversely, lower flow rates promote uniform dissolution, resulting in more predictable permeability changes (Luquot and Gouze, 2009; Michael et al., 2010).

Despite these advancements, challenges remain in understanding and optimizing the coupled effects of geochemical reactions, fluid dynamics, and rock properties.

In this study, an integrated modeling approach is employed to investigate the permeability changes induced by CO<sub>2</sub>-saturated brine injection in carbonate formations. The objectives of this study are:

- To quantify the impact of mineral dissolution and precipitation on porosity and permeability using reactive transport models.
- To validate the model predictions through laboratory experiments, including core flooding analysis.
- To optimize brine composition and injection parameters for enhanced injectivity and storage efficiency.

By combining experimental data with advanced modeling techniques, this study contributes to the understanding and optimization of CO<sub>2</sub> storage in deep saline aquifers, paving the way for more effective carbon capture, utilization, and storage (CCUS) strategies.

## 2 Materials and Methodology

### 2.1 Materials

The brine sample used in this study was synthetically made from laboratory-grade sodium chloride (NaCl) and potassium chloride (KCl) at 150°F, obtained from Fisher Scientific. The brine had a viscosity of 0.529 cp at 150°F. CO<sub>2</sub>-saturated brine was made by saturating the mentioned brine with CO<sub>2</sub> at 150°F and 1500 psi. A limestone core with 15.4% porosity and 19 mD permeability, obtained from the Indiana Limestone formation, was used as the porous media. Table 1, Table 2 and Table 3 list the chemical composition of brine, the properties of rock, and the 1D model condition respectively. The mineralogical composition of the limestone is characterized by X-ray diffraction (XRD).

Table 1: Chemical composition of brine.

Brine Species	Concentration (ppm)
Na <sup>+</sup>	31,485
K <sup>+</sup>	10,496
Cl <sup>-</sup>	58,045
TDS	100,000

Table 2: Properties of the outcrop limestone core.

Core	Diameter (in) x Length (in)	XRD Data
Limestone	1.5 × 2.8	99.5 wt% Calcite 0.5 wt% Quartz

Table 3: 1-D Model Parameters.

Parameter	Value
Initial porosity (%)	15.4
Initial permeability (mD)	19
Pressure (psia)	1500
Temperature (°F)	150

### 2.2 Core Flood Experiments

Core flood experiments were conducted by the laboratory to study the brine-limestone interactions at 150°F. Initially, the core was subjected to brine injection at the rate of 2 cc/min for 27.4 pore volumes. Next, the injection fluid was switched to CO<sub>2</sub>-saturated brine, with an injection rate of 0.07 cc/min for 45.8 pore volumes. The pressure difference was measured at each 1.2 pore volume of injection and permeability was calculated from the pressure difference using Darcy's law.

### 2.3 1D Model Description

An integrated model was used in this study to study the geochemical interactions of CO<sub>2</sub>-saturated brine with limestone during reactive, convective, and dispersive flow. The model combines PHREEQC, the geochemical software package developed by USGS (Parkhurst and Appelo, 2013), with the continuity equations to analyze the geochemical reactions and transport of flow in the porous media simultaneously.

PHREEQC has the capability of performing aqueous geochemical reactions including phase equilibrations and reactions, ion exchange, and surface complexations. Thus, this software can model dissolution/precipitation and ion exchange processes in a CO<sub>2</sub>-saturated brine/ limestone system.

Table 5 and Table 5 list the chemical reactions that are considered in the modeling. Ion exchange is crucial to be modeled here, since limestone as a carbonate rock has a negative surface charge (denoted by X in the reaction equations) and can interact with the cations of the brine, affecting the amount of dissolution/precipitation in the rock and leading to permeability alteration.

Table 4: List of dissolution/ precipitation reactions.

No.	Reaction	Log_k
1	$CaCO_3 \Leftrightarrow CO_3^{2-} + Ca^{2+}$	-8.48
2	$SiO_2 + 2H_2O \Leftrightarrow H_4SiO_4$	-3.75
3	$H_2O + CO_2 \Leftrightarrow H_2CO_3$	-1.47
4	$CaCO_3 + H_2CO_3 \Leftrightarrow Ca^{2+} + 2HCO_3^-$	6.68
5	$SiO_2 + H_2CO_3 \Leftrightarrow H_2SiO_3 + CO_2$	-3

Table 5: List of exchange reactions.

No.	Reaction	Log_k
1	$Na^+ + X^- \rightleftharpoons NaX$	0
2	$K^+ + X^- \rightleftharpoons KX$	0.5
3	$Ca^{2+} + 2X^- \rightleftharpoons CaX_2$	0.8

## 2.4 Model Workflow

By integrating PHREEQC with continuity equations, the model can dynamically adapt to real-time variations in the chemical and physical properties of the reservoir. Continuity equations, fundamental to dynamic modeling, govern the conservation of mass within a system. In the context of CO<sub>2</sub> storage, these equations are critical for simulating the flow of CO<sub>2</sub> and brine through porous media. When coupled with geochemical reactions, continuity equations enable the prediction of the transport and interaction of injected CO<sub>2</sub> with existing mineral species over time.

The integration of PHREEQC into the flow equation framework facilitates continuous model updates with current geochemical data, as illustrated in Figure 1. The modeling process begins with the initialization step, which establishes baseline reservoir conditions including porosity, permeability, pressure, temperature, and the initial chemical composition of the brine and rock matrix mineralogy. Following CO<sub>2</sub> injection, the continuity equations represent the distribution and flow of CO<sub>2</sub> and brine within the porous media.

Simultaneously, PHREEQC computes geochemical reactions at each time step, generating updated mineral saturation indices. These calculations allow the model to continuously assess changes in porosity and permeability based on the extent of mineral dissolution or precipitation. As minerals react, the pore spaces within the rock matrix are altered, affecting the structural and hydraulic properties of the reservoir.

Porosity evolution is continuously evaluated, and permeability adjustments are derived using the Carman-Kozeny equation. This approach quantitatively links changes in porosity to permeability, accounting for the dynamic interaction between geochemical reactions and reservoir properties. The Carman-Kozeny equation describes the evolution of porosity and permeability as shown in Equation 1 and Equation 2 below:

$$\frac{\partial \phi}{\partial t} = - \sum_{i=1}^n \frac{\phi}{\rho_i} \frac{\partial q_i}{\partial t} \tag{1}$$

Where,

$\phi$  : Porosity, fraction,

$\rho_i$  : Density of the mineral, mol/l (Calcite: 2.711 g/cc, Quartz: 2.65 gr/cc),

$q_i$ : Amount of reacted mineral, mol/L.

$$k = k_0 \left(\frac{\phi}{\phi_0}\right)^m \left(\frac{1-\phi_0}{1-\phi}\right)^2 \tag{2}$$

Where,

m: Carman-Kozeny exponent,

k and  $k_0$ : Current and original permeabilities,

$\phi$  and  $\phi_0$ : Current and original porosities.

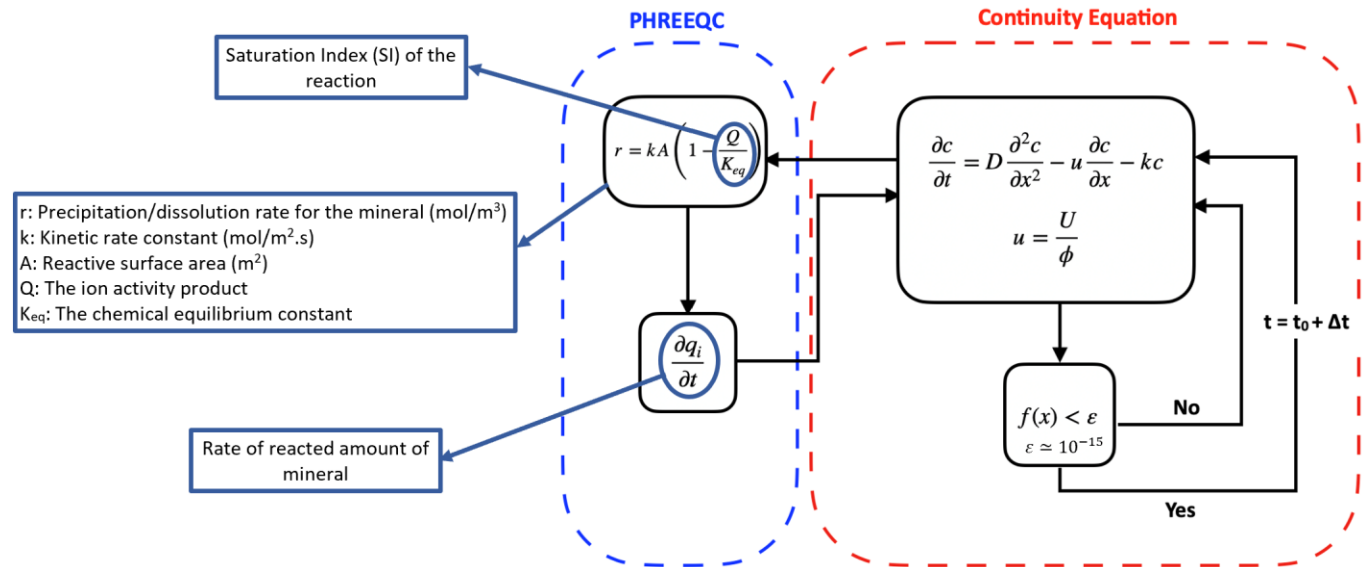


Figure 1: Coupled geochemical reactive workflow chart.

The impact of varying flow rates was analyzed within the model workflow using the Peclet number ( $Pe$ ) as a scaling parameter. High flow rates, indicated by high Peclet numbers, indicated convective transport within the system, resulting in enhanced geochemical reactions across a larger swept area.

Conversely, low flow rates, corresponding to reduced Peclet numbers, were characterized by dispersive flow, which facilitated the gradual and controlled dispersion of CO<sub>2</sub>. This slower process allowed for extended reaction times between CO<sub>2</sub> and the reservoir rock, promoting stable mineralization and long-term geochemical trapping.

The Peclet number is defined as:

$$Pe = \frac{Lu}{K} \quad (3)$$

Where,

L: Characteristic length (cm).

u: Velocity (cm/s).

K: Dispersion Coefficient (cm<sup>2</sup>/s).

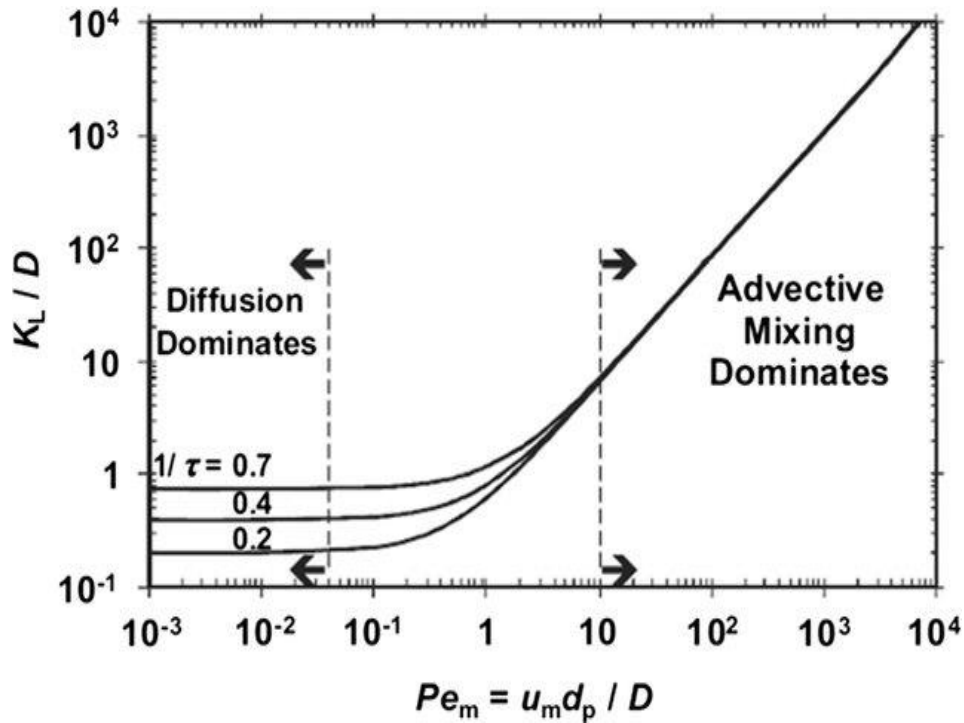


Figure 2: A schematic diagram illustrating the normalized dispersion coefficient as a function of the Peclet number for typical porous media with a grain size  $d_p$  (Hughes et al., 2012).

The normalized dispersion coefficient is schematically represented as a function of the Peclet number for typical porous media characterized by grain size ( $d_p$ ) in Figure 2. At low Peclet numbers, molecular diffusion predominates as the primary transport mechanism, while at high Peclet numbers, advective mixing becomes the dominant flow regime (Hughes et al., 2012). It is important to note that the threshold or transition zone between these two dominant physical mechanisms can vary substantially depending on the specific application.

### 3 Results

#### 3.1 Brine Injection

During brine injection, both quartz and calcite underwent dissolution; however, the extent of dissolution was negligible, as illustrated in Figures 3 and 4 and supported by Equations 1 and 2.

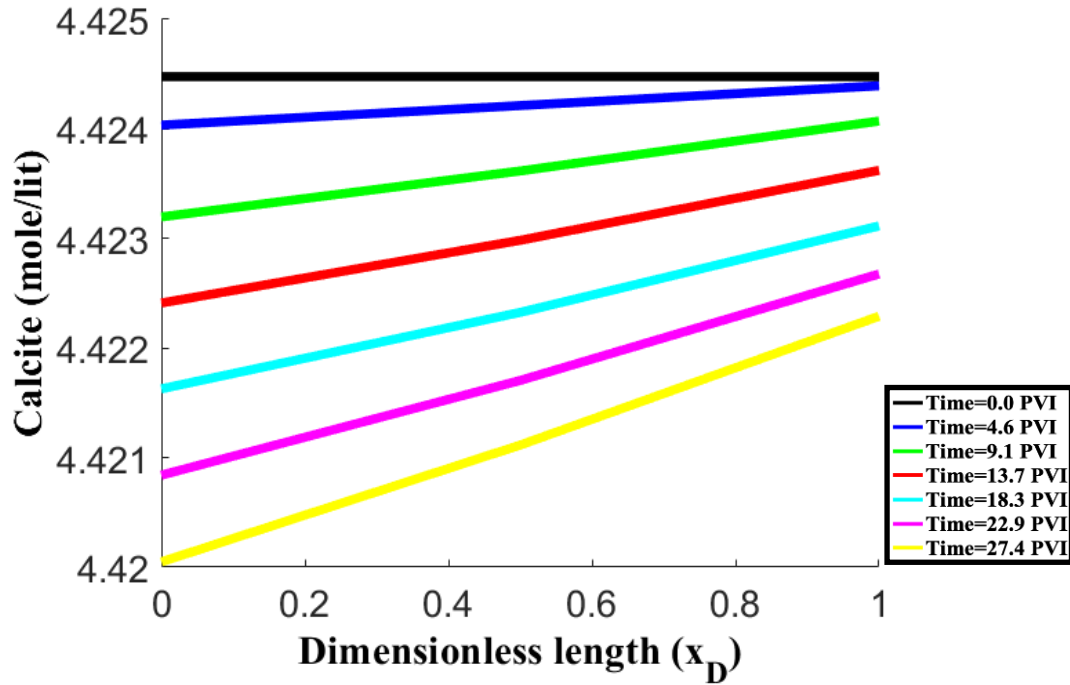


Figure 3: Calcite concentration vs. dimensionless length.

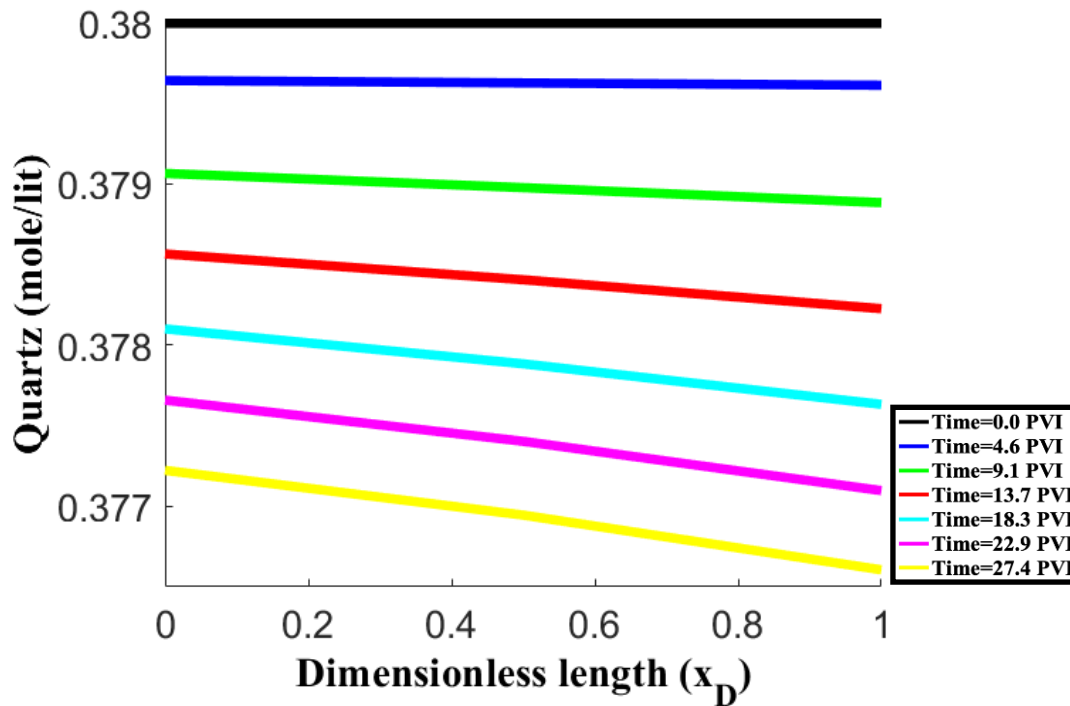


Figure 4: Quartz concentration vs. dimensionless length.

Figure 5 shows the concentrations of  $\text{Na}^+$ ,  $\text{K}^+$ , and  $\text{Cl}^-$  in the effluent. After approximately 6 pore volumes of injection, these concentrations returned to their initial levels in the injected brine, indicating that the brine is non-reactive in this porous medium mainly composed of calcite and quartz.

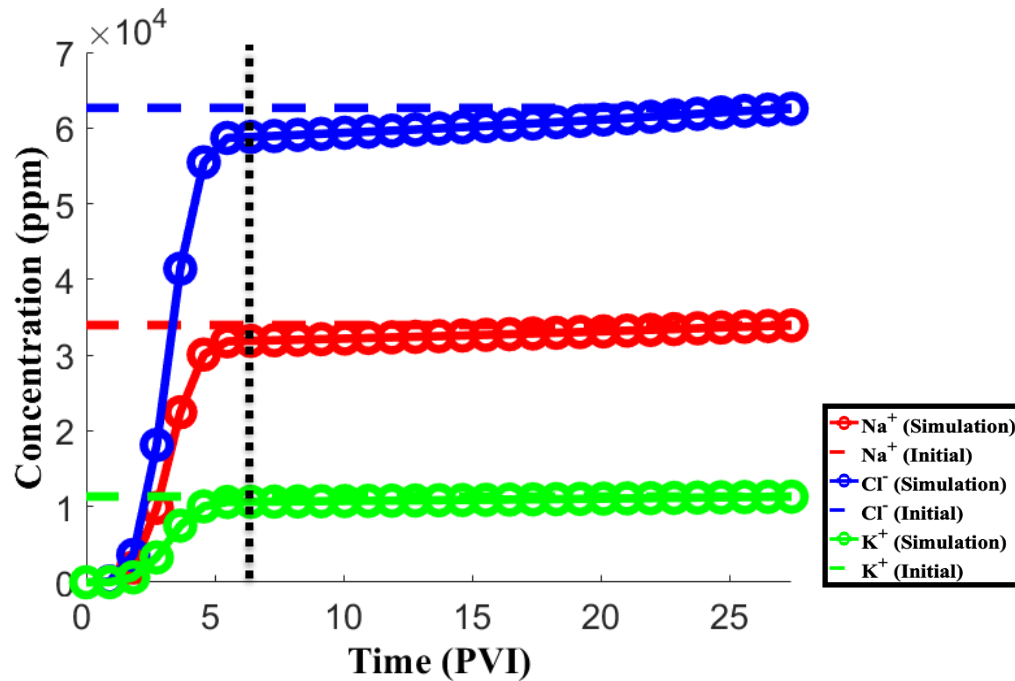


Figure 5: Effluent composition vs. pore volume injected.

These are the main reasons why the porosity and permeability of the system remained unchanged after brine injection. As shown in Figures 6 and 7, the porosity changed by approximately 0.01%, resulting in an almost stable permeability (Please note that the vertical axis of Figure 7 has been adjusted to magnify the permeability changes for better readability).

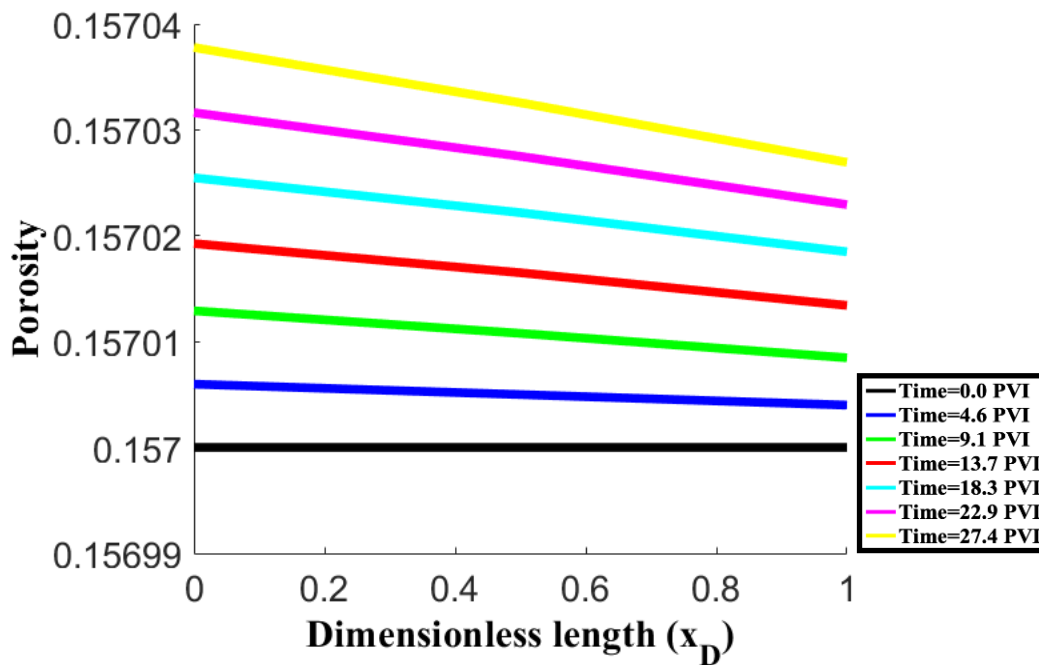


Figure 6: Porosity vs. dimensionless length.



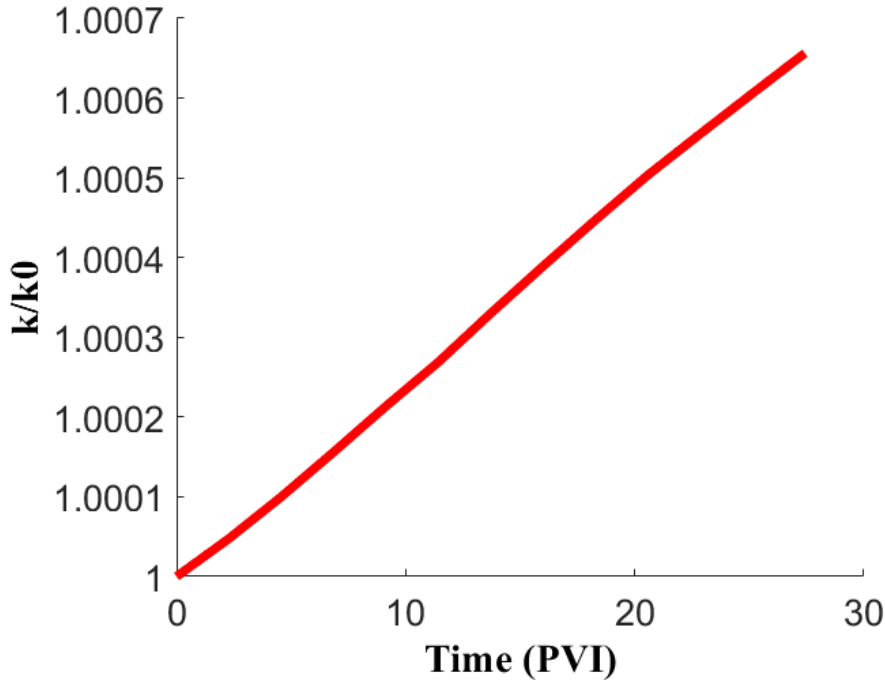


Figure 7: Permeability ratio ( $k/k_0$ ) vs. pore volume injected.

### 3.2 CO<sub>2</sub>- Saturated Brine Injection

After CO<sub>2</sub>-saturated brine injection, Calcite dissolves until a specific pore volume injected (PVI) is reached, after which it begins to precipitate. According to the modeling, calcite precipitation starts at a PVI of 17 (Figure 8). The change in the trend could be attributed to the brine becoming saturated with HCO<sub>3</sub><sup>-</sup>, as one of the products of CO<sub>2</sub>-saturated brine. Additionally, the brine could be saturated with Ca<sup>2+</sup>, as Calcite kinetics is fast, and equilibrium is achieved within a few days (this is justifiable based on Equation 4).

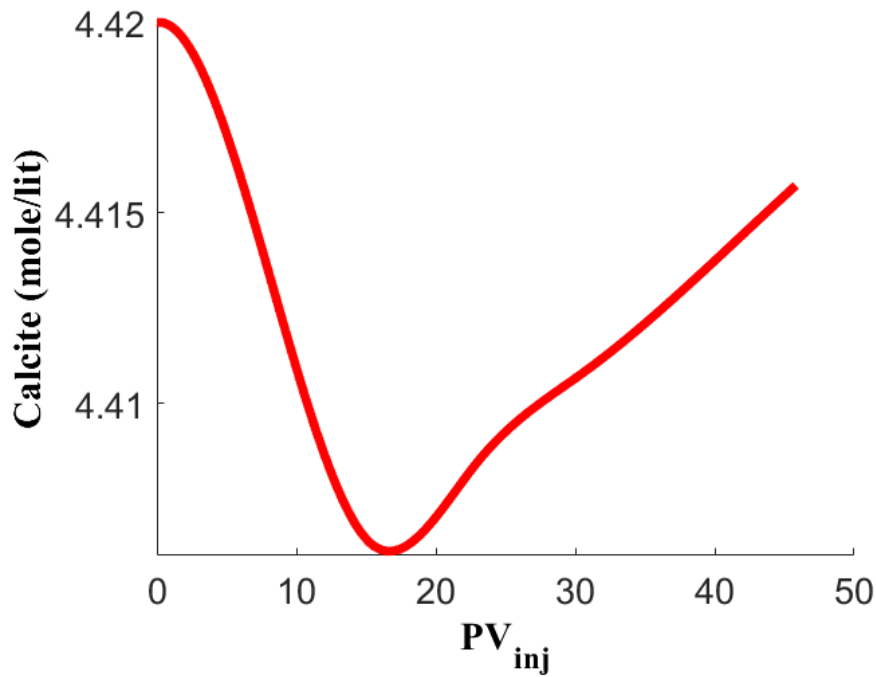


Figure 8: Calcite concentration vs. pore volume injected.

Unlike Calcite, Quartz dissolved consistently without any precipitation during the injection of CO<sub>2</sub>-saturated brine, as shown in Figure 9.

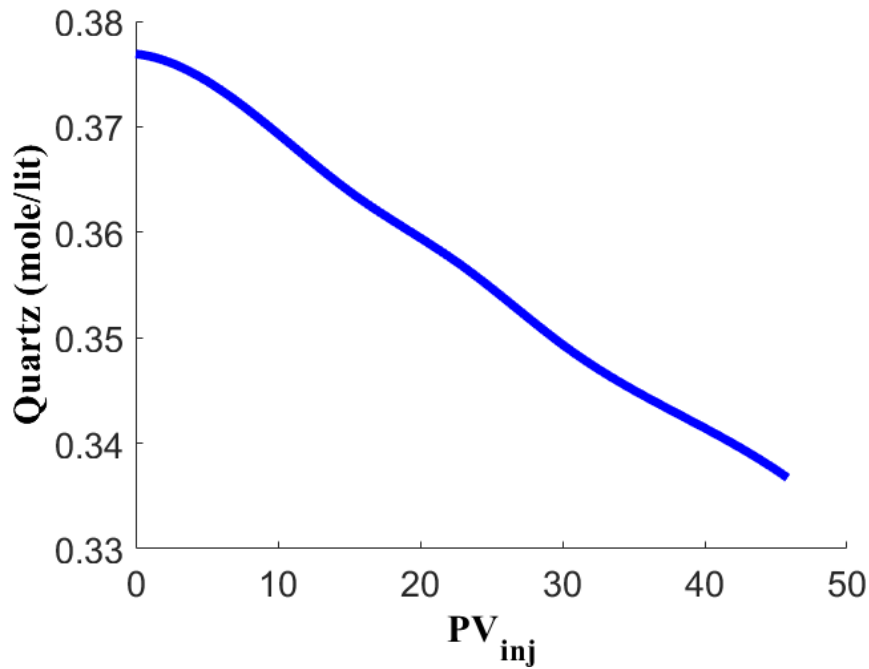


Figure 9: Quartz concentration vs. pore volume injected.

As shown in Figure 10 and based on the reasons mentioned for each mineral's interaction with CO<sub>2</sub>-saturated brine, the total rock mineral composition (calcite + quartz) undergoes dissolution at this phase.

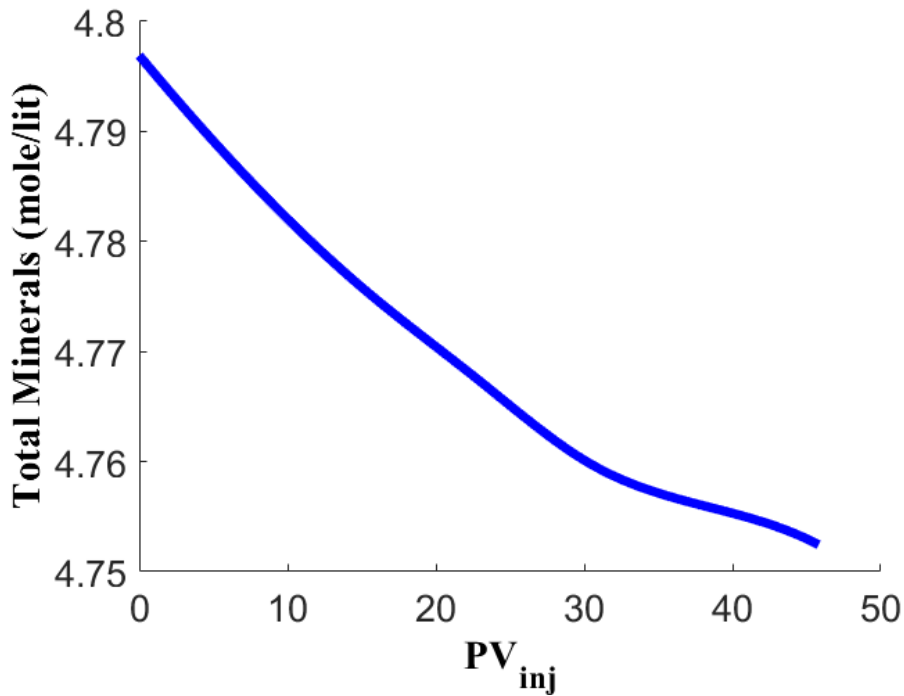


Figure 10: Total rock mineral concentration vs. pore volume injected.

Figure 11 illustrates the concentrations of Na<sup>+</sup>, K<sup>+</sup>, and Cl<sup>-</sup> in the effluent, with ion stabilization occurring after approximately 72 pore volumes of injection. This indicates that saturating the brine with CO<sub>2</sub> increases the time required for system stabilization. In other words, CO<sub>2</sub>-saturated brine acts as a reactive flow within this system.

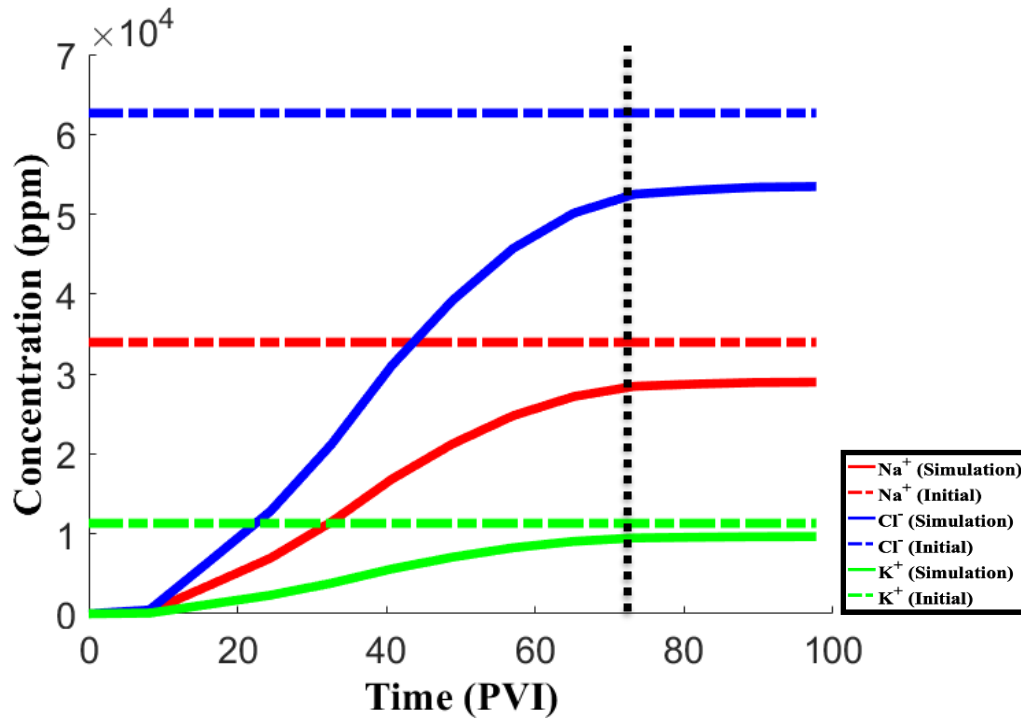


Figure 11: Effluent composition vs. pore volume injected.

Due to the factors and mechanisms previously discussed, such as the net rock dissolution and surface ion exchange reactions, after injecting CO<sub>2</sub>-saturated brine for 45.8 pore volumes (PVs), the porosity increased by as much as 5% (Figure 12). Additionally, the permeability increased to nearly 2.5 times its initial value (Figure 13).

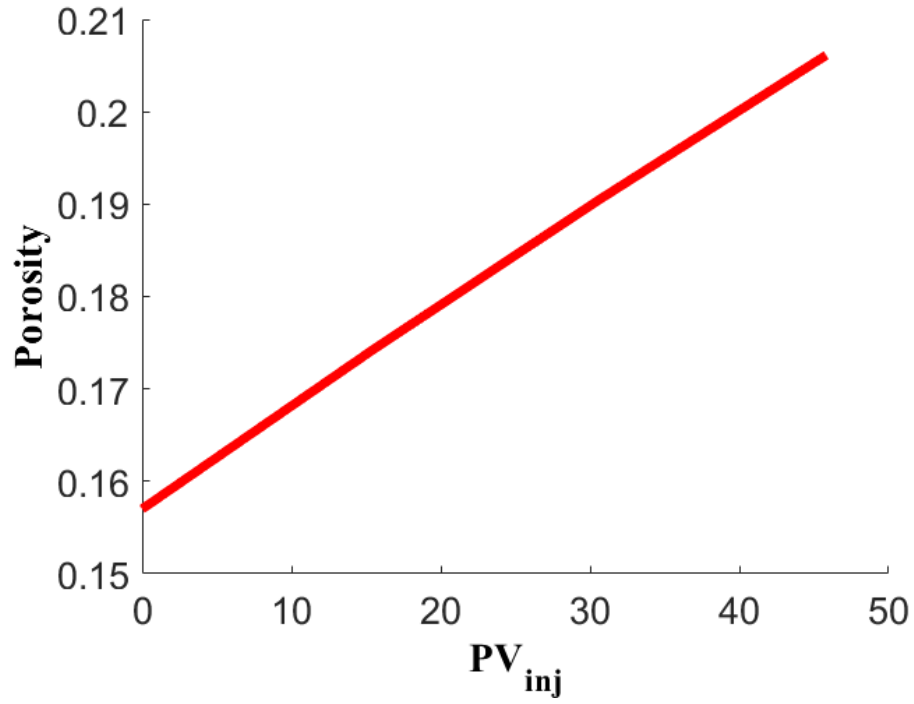
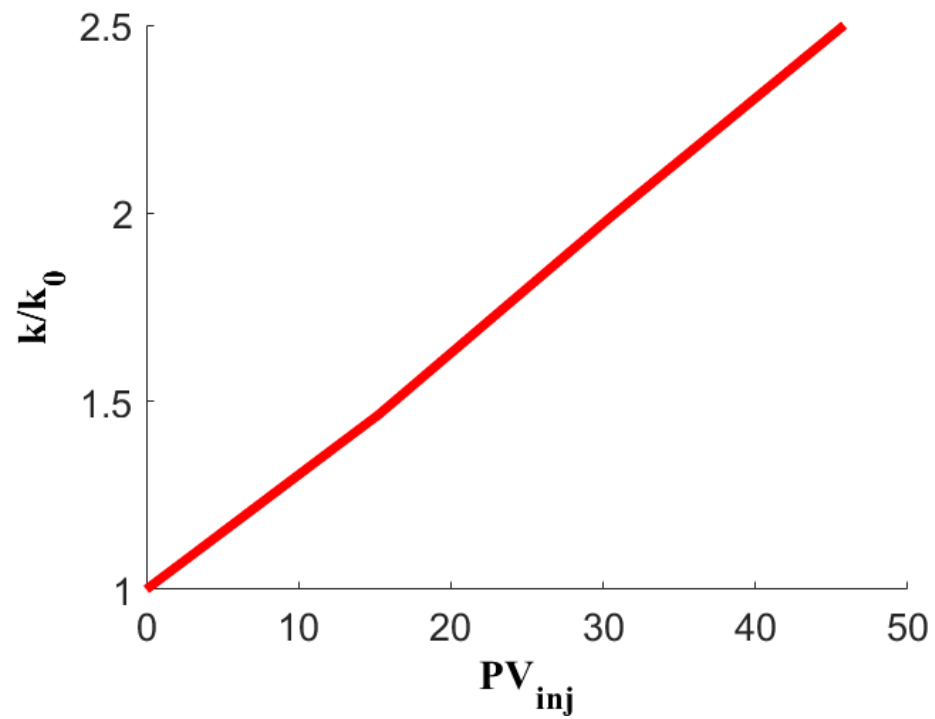


Figure 12: Porosity vs. pore volume injected.

Figure 13: Permeability ratio ( $k/k_0$ ) vs. pore volume injected.

### 3.3 Model Validation with Experimental Data

Figure 14 compares the modeling results (depicted by the red line) with the experimental data (represented by the blue dots). As shown in Figure 14, the modeling results closely align with the experimental data.

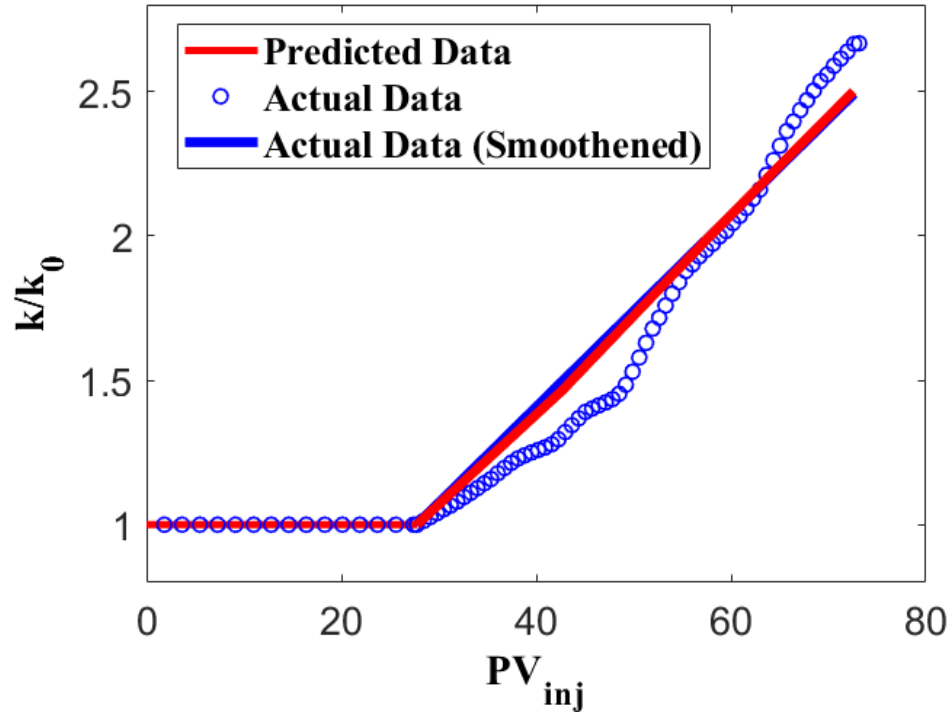


Figure 14: Permeability ratio ( $k/k_0$ ) vs. pore volume injected (experiment vs simulation data)

### Conclusions

- Storing  $\text{CO}_2$  in deep saline aquifers, as a solution for greenhouse gas reduction, highly depends on the storage capacity of the aquifer. This capacity is a function of permeability changes, especially near the well, caused by  $\text{CO}_2$ /brine/rock interactions. As a result, the footprint (well-count) of the injection is impacted by the injectivity, and thus how the  $\text{CO}_2$  propagates in the system.
- To simulate the permeability changes, a 1-D in-house model has been developed in this study to investigate mineralization in deep saline aquifers after  $\text{CO}_2$ -saturated brine injection and/or exposure of the rock where the  $\text{CO}_2$  solution mechanism takes place and thus the property changes in the rock-fabric.
- Brine injection minimally impacts permeability, even at higher pore volume injections. Conversely, injecting  $\text{CO}_2$ -saturated brine into the rock composed of Calcite and Quartz (or exposing the rock to  $\text{CO}_2$ -saturated brine at the plume interface) leads to a notable permeability increase, doubling the original value of the permeability due to the system-scale mineral dissolution.
- The complex interplay between injection fluids and rock composition highlights the importance of considering geological formations in  $\text{CO}_2$  storage assessments. In the lab, by manipulating brine composition and further saturating it with  $\text{CO}_2$ , the optimum brine composition is attainable. Sensitivity analysis on the rock composition helps in targeting suitable rocks for CCS under operational conditions, reducing formation damage risk and sensitivity analysis.

## Acknowledgment

The research described here was supported mainly by Core Laboratories CCUS Consortium, in addition, by the members of the Research Consortium on Interaction of Phase Behavior and Flow (IPB&F) Consortium.

## References

- Abdulwarith, A., Ammar, M. and Dindoruk, B., 2024a. Prediction/Assessment of CO<sub>2</sub> EOR and Storage Efficiency in Residual Oil Zones Using Machine Learning Techniques, SPE/AAPG/SEG Carbon, Capture, Utilization, and Storage Conference and Exhibition. SPE, pp. D031S022R002.
- Abdulwarith, A., Kareb, A., Ammar, M. and Dindoruk, B., 2024b. Evaluation of cyclic gas injection EOR in unconventional reservoirs and exit strategies, including potential storage options using Bakken Field as an example case, Unconventional Resources Technology Conference, 17–19 June 2024. Unconventional Resources Technology Conference (URTeC), pp. 1705-1727.
- Addassi, M. et al., 2022. Assessing the potential of solubility trapping in unconfined aquifers for subsurface carbon storage. *Scientific Reports*, 12(1): 20452.
- Ammar, M. et al., 2024. Case Study of Gas Flaring Mitigation Through Optimized Gas Re-Injection While Improving the Recovery in High-Temperature Offshore Reservoirs, SPE Improved Oil Recovery Conference? SPE, pp. D031S013R003.
- Bachu, S., 2015. Review of CO<sub>2</sub> storage efficiency in deep saline aquifers. *International Journal of Greenhouse Gas Control*, 40: 188-202.
- Hughes, T.J. et al., 2012. CO<sub>2</sub> sequestration for enhanced gas recovery: New measurements of supercritical CO<sub>2</sub>–CH<sub>4</sub> dispersion in porous media and a review of recent research. *International Journal of Greenhouse Gas Control*, 9: 457-468.
- Jahediesfanjani, H., Anderson, S.T. and Warwick, P.D., 2019. Improving pressure-limited CO<sub>2</sub> storage capacity in saline formations by means of brine extraction. *International Journal of Greenhouse Gas Control*, 88: 299-310.
- Kampman, N., Bickle, M., Wigley, M. and Dubacq, B., 2014. Fluid flow and CO<sub>2</sub>–fluid–mineral interactions during CO<sub>2</sub>-storage in sedimentary basins. *Chemical Geology*, 369: 22-50.
- Li, L., Zhao, N., Wei, W. and Sun, Y., 2013. A review of research progress on CO<sub>2</sub> capture, storage, and utilization in Chinese Academy of Sciences. *Fuel*, 108: 112-130.
- Luquot, L. and Gouze, P., 2009. Experimental determination of porosity and permeability changes induced by injection of CO<sub>2</sub> into carbonate rocks. *Chemical geology*, 265(1-2): 148-159.
- Michael, K. et al., 2010. Geological storage of CO<sub>2</sub> in saline aquifers—A review of the experience from existing storage operations. *International journal of greenhouse gas control*, 4(4): 659-667.
- Noiriel, C. et al., 2009. Changes in reactive surface area during limestone dissolution: An experimental and modelling study. *Chemical Geology*, 265(1-2): 160-170.
- Parkhurst, D.L. and Appelo, C., 2013. Description of input and examples for PHREEQC version 3—a computer program for speciation, batch-reaction, one-dimensional transport, and inverse geochemical calculations. *US geological survey techniques and methods*, 6(A43): 497.
- Xu, T., Apps, J.A. and Pruess, K., 2004. Numerical simulation of CO<sub>2</sub> disposal by mineral trapping in deep aquifers. *Applied geochemistry*, 19(6): 917-936.

Appendix:

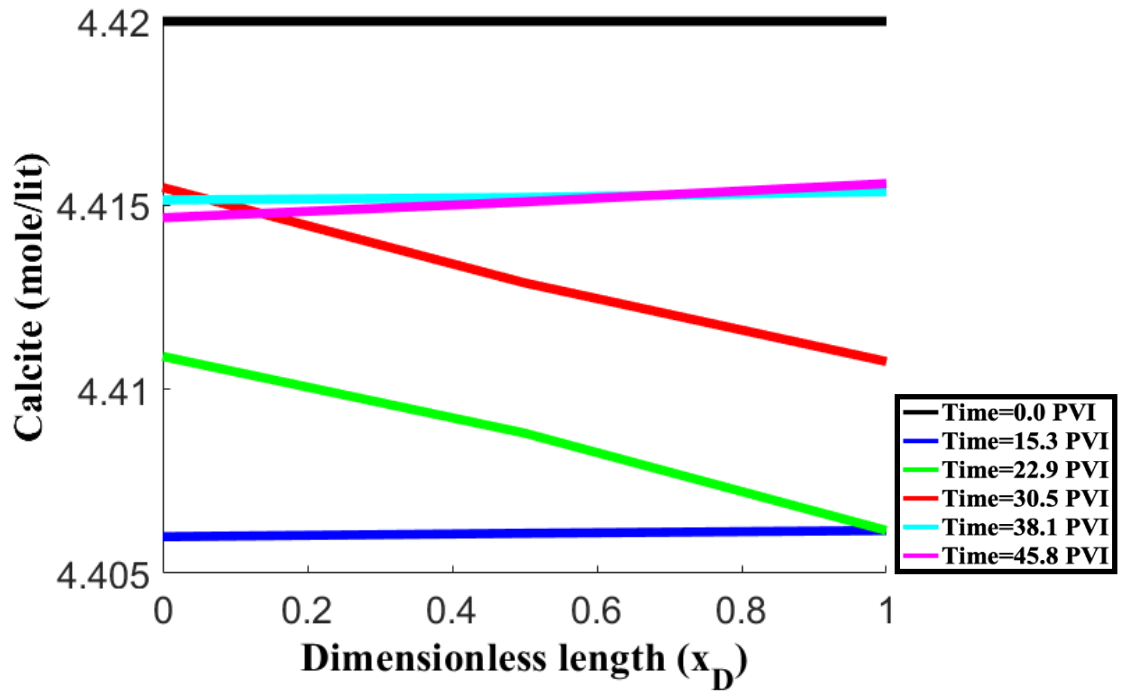


Figure 1-A: Quartz concentration vs. dimensionless length.

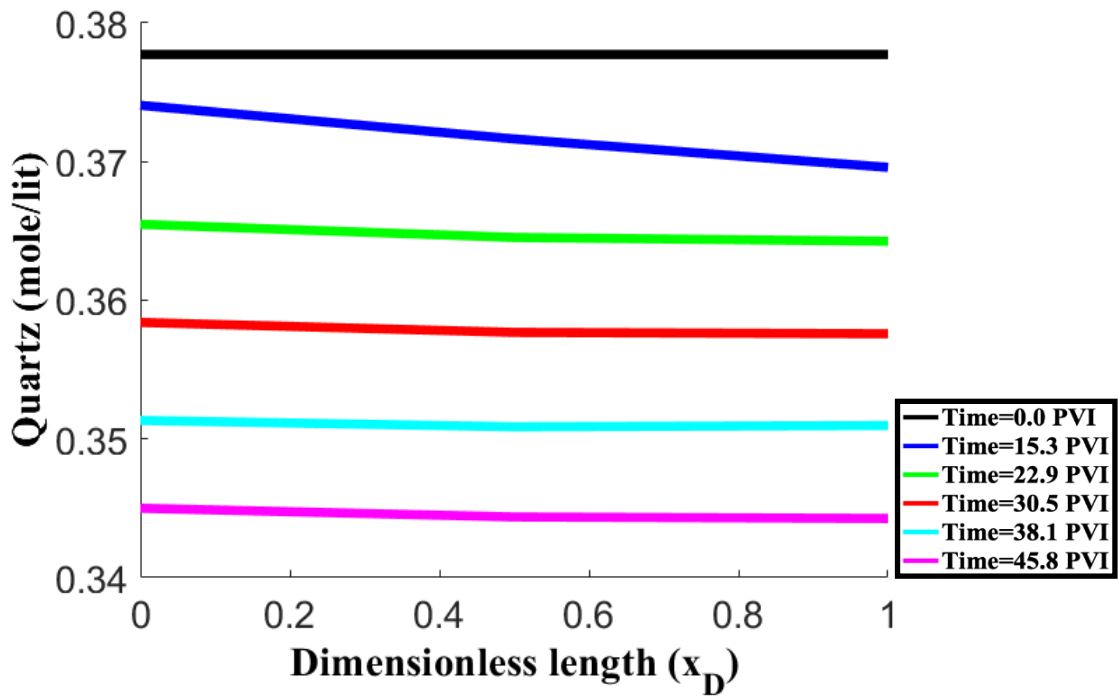


Figure 2-A: Calcite concentration vs. dimensionless length.

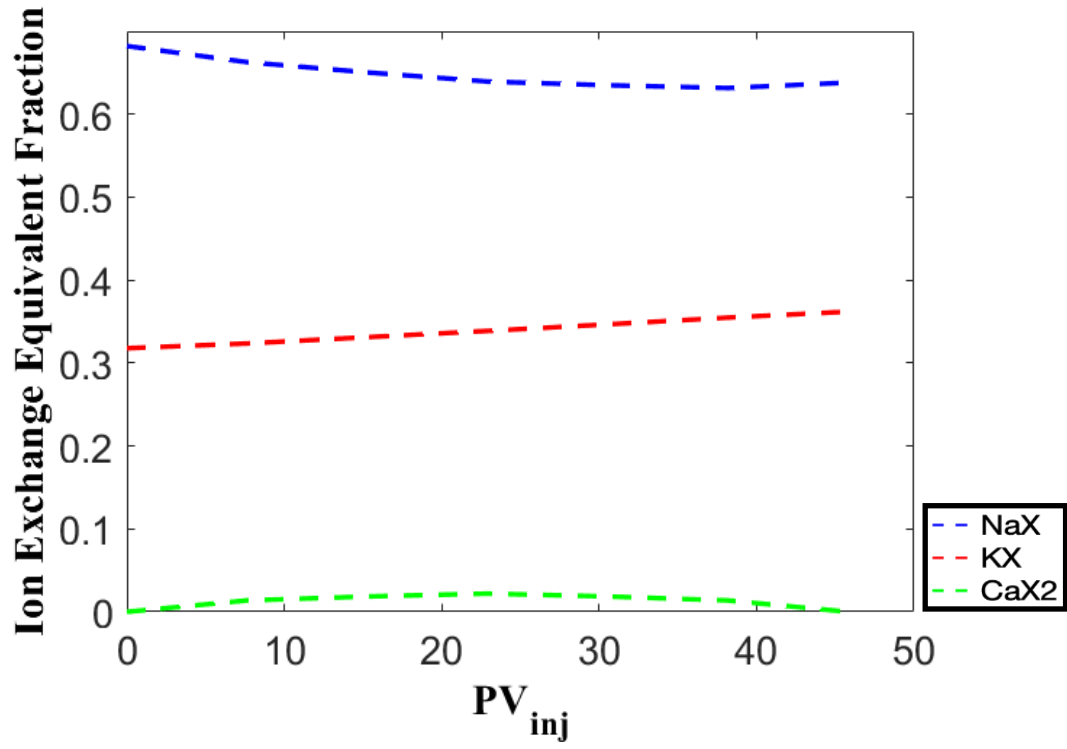


Figure 3-A: Surface complex vs. pore volume injected.